Bang-Bang Evasion: Its Stochastic Optimality and a Terminal-Set-Based Implementation

Liraz Mudrik*
Naval Postgraduate School, Monterey, CA, 93943

Yaakov Oshman[†]
Technion—Israel Institute of Technology, Haifa, 3200003, Israel

We address the problem of optimal evasion in a planar endgame engagement, where a target with bounded lateral acceleration seeks to avoid interception by a missile guided by a linear feedback law. Contrary to existing approaches, that assume perfect information or use heuristic maneuver models in stochastic settings, we formulate the problem in an inherently stochastic framework involving imperfect information and bounded controls. Complying with the generalized separation theorem, the control law factors in the posterior distribution of the state. Extending the well-known optimality of bang-bang evasion maneuvers in deterministic settings to the realm of realistic, stochastic evasion scenarios, we firstly prove that an optimal evasion strategy always exists, and that the set of optimal solutions includes at least one bang-bang policy, rendering the resulting optimal control problem finite-dimensional. Leveraging this structure, we secondly propose the closed-loop terminal-set-based evasion (TSE) strategy, and demonstrate its effectiveness in simulation against a proportional navigation pursuer. Monte Carlo simulations show that the TSE strategy outperforms traditional stochastic evasion strategies based on random telegraph, Singer, and weaving models.

---

*Postdoctoral Fellow, Dept. of Mechanical and Aerospace Engineering. Member AIAA. Email: `liraz.mudrik.ctr@nps.edu`. This work is part of Dr. Mudrik's doctoral research, performed at the Technion—Israel Institute of Technology, Haifa, 3200003, Israel.

[†]Professor Emeritus, Stephen B. Klein Faculty of Aerospace Engineering. Fellow AIAA. `yaakov.oshman@technion.ac.il`.

I. Introduction

At the terminal phase of an interception scenario, a defending aerial vehicle must perform evasive maneuvers to avoid an attacking missile. This work considers such engagements in the commonly used planar lateral engagement, where the interceptor uses a state-feedback guidance law to home in on a maneuvering target. The optimal design of interceptor guidance laws has been extensively studied under deterministic settings, leading to canonical strategies such as proportional navigation (PN), augmented PN (APN), the optimal guidance law (OGL) [1], and the linear-quadratic differential game (LQDG) guidance law [2]. These strategies arise from linearized engagement dynamics and quadratic cost functionals and thus induce linear acceleration commands.

From the evader's perspective, the optimal maneuver against such linear guidance laws, under bounded acceleration constraints, has been shown to be of bang-bang form, i.e., switching between the minimal and maximal allowable control inputs. This structure was first demonstrated for evasion from PN-guided missiles in both two-dimensional [3, 4] and three-dimensional [5] settings. Later, Shima [6] generalized the result to cover a broad class of linear guidance laws, including PN, APN, and OGL, showing that the evader's optimal response remains bang-bang. These findings were extended to more realistic scenarios by incorporating estimator-based inference. In particular, Fonod and Shima [7] employed a multiple model adaptive estimator (MMAE) [8] to identify the interceptor's guidance law from a known library and applied the corresponding bang-bang optimal evasion policy. Subsequently, Turetsky and Shima [9] showed that the bang-bang form persists even when the interceptor switches its guidance law mid-engagement, regardless of whether the switching time is known to the target. Later, Shaferman [10] demonstrated that bang-bang maneuvers remain optimal even when the target exploits estimation delays in the interceptor's guidance loop [11]. Recent works further highlight the prevalence of structured optimal evasion in adversarial and uncertain settings. In particular, [12] analyzed three-dimensional bang-bang maneuvers without knowledge of the interceptor's guidance law based on the kinematics and engagement geometry, while [13] derived closed-form optimal evasive strategies against general linear-quadratic-optimal guidance laws. However, all of these studies remain deterministic and assume perfect information,

in which both agents possess complete knowledge of their own and their opponent's states.

In realistic scenarios, the evader must instead estimate the interceptor's state through noisy measurements. This motivates a stochastic formulation of the evasion problem. When modeling such systems, particularly under bounded controls and potentially non-Gaussian uncertainties, it is appropriate to adopt the generalized separation theorem (GST), originally stated by Witsenhausen [14] and derived from Striebel's sufficiency results [15]. The GST allows for the estimator to be designed separately, whereas the controller uses the posterior distribution of the system state as computed by the estimator.

In stochastic evasion settings, where full information about the states is unavailable, evader behavior is often modeled using randomized or probabilistic control profiles. Commonly used examples include the random telegraph signal (RTS) model, where the target arbitrarily switches between the maximal and minimal acceleration commands [1, 16], the Singer process [17], in which acceleration follows a first-order Gauss–Markov process with finite correlation time, and weaving maneuvers where the evader performs sinusoidal motion [1]. Variants of the weaving model have been extensively studied, e.g., in [18–21], often in the context of assessing guidance system robustness or estimator adaptation. Although RTS, Singer, and weaving models are useful for evaluating interceptor performance, they are generally heuristic and do not yield provably optimal feedback evasion strategies under stochastic uncertainty. Moreover, prior stochastic evasion models lacked a proof of optimal feedback form under uncertainty.

This work addresses that gap by studying the optimal evasion problem for a bounded-control evader operating under uncertainty about the engagement's state. We formulate the problem in discrete time following the GST lines, where a posterior distribution represents the imperfect information about the states. Our first and main contribution is a general existence result: we prove that an optimal evasion policy exists, and that there is at least one such policy with a bang-bang structure. This extends the well-known deterministic result to the stochastic setting and establishes that the structure of optimal evasive maneuvers remains extremal even under uncertainty. Importantly, this result reduces the complexity of optimal evasion synthesis from an infinite-dimensional control

space to a finite one, albeit still requiring a considerable computational cost.

Having proved the main, general result, we then use it to introduce our second contribution, which is a specific evasion policy based on the notion of terminal sets. The idea of using such sets for guidance problems was first presented in [22], where the pursuer's guidance law was devised using sequential Monte Carlo (MC) techniques. Later, [23] showed how this approach can be evaluated analytically in a linearized-Gaussian setting. This policy leverages the bang-bang structure to select between the extremals at each time step based on predicted terminal outcomes derived from state estimates. We demonstrate its efficacy in simulation against a proportional navigation-guided pursuer and benchmark its performance against the RTS, Singer, and weaving models commonly used in the stochastic guidance literature.

The remainder of this paper is organized as follows. Section II formulates the problem and modeling assumptions. The first and main contribution of the paper is introduced in Section III, which formulates and proves the existence theorem. Section IV presents the second contribution of the paper, that is, the terminal-set-based evasion (TSE) strategy with conventional stochastic models. Section V presents simulation results of the TSE, including comparison with the RTS, Singer, and weaving evasion models. Concluding remarks are offered in Section VI.

II. Problem Formulation

A linearized, pursuer-evader stochastic engagement scenario is considered. The problem is mathematically formulated in the sequel.

A. Linearized Kinematics and Dynamics

Figure 1 shows a schematic view of the geometry of the assumed planar endgame scenario, where X-Y is a Cartesian inertial reference frame. The intercepting missile and the target are denoted by M and T, respectively. Variables associated with the interceptor and the target are denoted by additional subscripts M and T, respectively. The speed, normal acceleration, and the path angle are denoted by V, a, and γ, respectively. The slant range between the pursuer and the evader is ρ,

and the line of sight (LOS) angle, measured from the X_I axis, is λ. We linearize the trajectories of the interceptor and the target along the initial LOS. Commonly used in guidance strategies, the interceptor and target accelerations normal to the initial LOS are denoted by $\grave{a}_M$ and $\grave{a}_T$, respectively. These accelerations satisfy the following relations

$$\grave{a}_M = a_M \cos(\gamma_M^0 - \lambda^0) \tag{1}$$

$$\grave{a}_T = a_T \cos(\gamma_T^0 + \lambda^0). \tag{2}$$

Variables with superscript 0 are initial values, about which the linearization is performed.
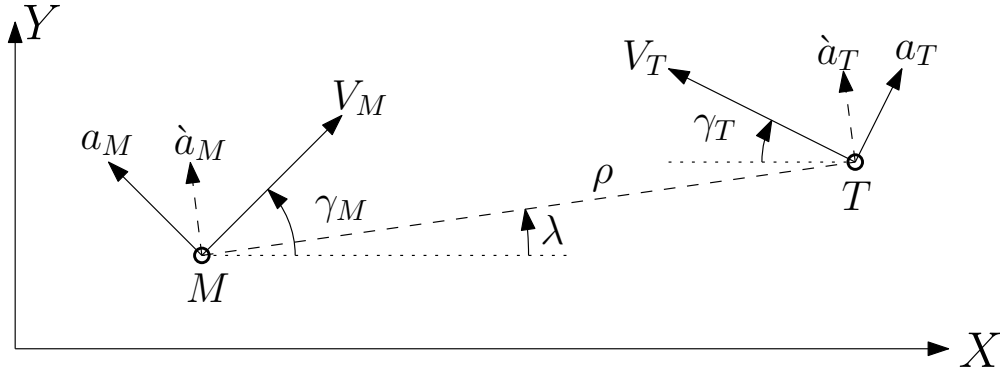

Fig. 1   Planar engagement geometry

In this scenario, we assume that the interceptor and the target can be represented as point masses, and that the target's own path angle and lateral acceleration are known (e.g., via its navigation system). It is also assumed that the speeds of both the interceptor and the target, V_M and V_T, respectively, are known and time-invariant. The lateral acceleration command of the target is assumed to be bounded by a known constant, $u_T^{\max}$.

We define the state vector as

$$\mathbf{x} = \begin{bmatrix} \xi & \dot{\xi} & \mathbf{q}_M^\top & \mathbf{q}_T^\top \end{bmatrix}^\top \in \mathbb{R}^{n_x} \tag{3}$$

where $\mathbf{q}_M^\top$ and $\mathbf{q}_T^\top$ are the state vectors of internal dynamics of the interceptor and the target, respectively. We assume that their closed-loop dynamics can be represented via a known, arbitrary-

order linear system. The discrete-time equations of motion (EOM) are

$$\mathbf{x}^{k+1} = \mathbf{F}^k(\eta)\mathbf{x}^k + \mathbf{g}_M^k(\eta)u_M^k + \mathbf{g}_T^k u_T^k + \omega^k \tag{4}$$

where ω^k is a white process noise with a known probability density function (PDF) p_{ω^k} and η is a random vector representing uncertain parameters of the interceptor dynamics, which also has a known PDF p_η. We also assume that the process noise and the uncertain parameters are statistically independent. The process noise is used to stochastically model the effects of physical phenomena that cannot be modeled deterministically, e.g., turbulence. The vector of uncertain parameters can be used to handle imprecise knowledge about specific parameters, such as those associated with the interceptor's dynamics, as described in the following example.

Example II.1. *Assume that both sides possess strictly proper first-order maneuvering dynamics, and define the state vector as*

$$\mathbf{x} = \begin{bmatrix} \xi & \dot{\xi} & \grave{a}_M & \grave{a}_T \end{bmatrix}^\top \tag{5}$$

Using a zero-order hold discretization over the interval $(t^k, t^k + \Delta t]$ results in the following EOM

$$\mathbf{F}_M^k = \begin{bmatrix} 1 & \Delta t & -\tau_M^2 \psi\left(\frac{\Delta t}{\tau_M}\right) & \tau_T^2 \psi\left(\frac{\Delta t}{\tau_T}\right) \\ 0 & 1 & -\tau_M\left(1 - e^{-\frac{\Delta t}{\tau_M}}\right) & \tau_T\left(1 - e^{-\frac{\Delta t}{\tau_T}}\right) \\ 0 & 0 & e^{-\frac{\Delta t}{\tau_M}} & 0 \\ 0 & 0 & 0 & e^{-\frac{\Delta t}{\tau_T}} \end{bmatrix}, \quad \mathbf{g}_M = \begin{bmatrix} -\tau_M^2 \Upsilon\left(\frac{\Delta t}{\tau_M}\right) \\ -\tau_M \psi\left(\frac{\Delta t}{\tau_M}\right) \\ 1 - e^{-\frac{\Delta t}{\tau_M}} \\ 0 \end{bmatrix}, \quad \mathbf{g}_T = \begin{bmatrix} \tau_T^2 \Upsilon\left(\frac{\Delta t}{\tau_T}\right) \\ \tau_T \psi\left(\frac{\Delta t}{\tau_T}\right) \\ 0 \\ 1 - e^{-\frac{\Delta t}{\tau_T}} \end{bmatrix} \tag{6}$$

where

$$\psi(t) = e^{-t} + t - 1, \tag{7}$$

$$\Upsilon(t) = \frac{1}{2}t^2 - e^{-t} - t + 1. \tag{8}$$

In this case, τ_M is an uncertain parameter for the target. Assuming that $\tau_M \in [\tau_M^{\min}, \tau_M^{\max}]$, where

$\tau_M^{\min}$ and $\tau_M^{\max}$ are known, we can set $\eta \sim U[\tau_M^{\min}, \tau_M^{\max}]$.

B. Engagement Duration

The final time is commonly approximated as

$$t^f \approx \frac{\rho^0}{V_M \cos(\gamma_M^0 - \lambda^0) + V_T \cos(\gamma_T^0 + \lambda^0)} \tag{9}$$

where ρ^0 is the initial range. This approximation precludes any deviations from the collision course, and, furthermore, it assumes that the initial range is perfectly known. Circumventing the latter problem, we follow [24] and model the final time-step, f, which is the nearest integer to $t^f/\Delta t$, as a random variable with a known probability mass function (PMF), $p_f(i)$ for all $i = 0, 1, \ldots, \infty$. As the horizon of engagement scenarios is finite, $f < \infty$ almost surely, yielding that there exists $i' < \infty$ such that

$$\sum_{i=i'}^{\infty} p_f(i) = 0. \tag{10}$$

This allows defining the time-to-go at time t^k as $t_{go}^k \triangleq \Delta t(f - k)$. This variable is also random, and its PMF satisfies

$$p_{t_{go}^k}(i) = \frac{p_f(i/\Delta t + k)}{\sum_{i=0}^{\infty} p_f(i/\Delta t + k)}, \qquad \forall i = 0, 1, \ldots, \infty, \qquad \forall k = 0, \ldots, k', \tag{11}$$

where k', the maximal value of k for which (11) is defined, solves

$$\max_{k \in \{0,1,\ldots,\infty\}} k$$
$$\text{s.t.} \quad \sum_{i=0}^{\infty} p_f(i/\Delta t + k) > 0. \tag{12}$$

Note that the normalization factor is required in cases where

$$\sum_{i=0}^{k-1} p_f(i) > 0. \tag{13}$$

For any k that nullifies this summation we can use $p_{t_{go}^k}(i) = p_f(i/\Delta t + k)$ for all $i = 0, 1, \ldots, \infty$.

C. Estimation

Following the guidelines of the GST, we assume that a state estimator is designed independently. Using noisy measurements, the estimator outputs a posterior PDF of the state vector, denoted as p_{x^k}, at every Δt seconds, according to

$$y^k = h(\mathbf{x}^k) + v^k \tag{14}$$

where v^k is a white measurement noise with a known PDF p_{v^k} and $h(\cdot)$ is a given measurement function. For example, [7] uses the MMAE estimator to both estimate the interceptor's state and identify its guidance law when the measurement function is linear and the driving noises are Gaussian.

Because this work focuses on the structure of the control law of the evader, we assume that the estimation problem has already been solved, and, hence, that the posterior PDF of the state vector (3) is available.

D. Pursuer Guidance Strategy

1. Linear Guidance Laws

This work considers evasion from a pursuer that uses a linear guidance law. Linear laws result from solving linear-quadratic formulations of optimal control or differential game problems. These laws are commonly represented by the structure:

$$u_M = \frac{\mathcal{N}_p z_p}{t_{go}^2}, \qquad p \in \mathcal{P} \tag{15}$$

where $\mathcal{N}$ and z are the navigation gain and the zero-effort miss (ZEM) of each guidance law, respectively, and $\mathcal{P}$ is the set of possible guidance laws used by the pursuer. Using the state

vector (5), we present the following noteworthy examples for the ZEM:

$$z_{\text{PN}} = x_1 + x_2 t_{go} \tag{16a}$$

$$z_{\text{APN}} = x_1 + x_2 t_{go} + \frac{1}{2} t_{go}^2 x_4 \tag{16b}$$

$$z_{\text{OGL}} = x_1 + x_2 t_{go} - \tau_M^2 \psi(t_{go}/\tau_M) x_3 + \frac{1}{2} t_{go}^2 x_4 \tag{16c}$$

$$z_{\text{LQDG}} = x_1 + x_2 t_{go} - \tau_M^2 \psi(t_{go}/\tau_M) x_3 + \tau_T^2 \psi(t_{go}/\tau_T) x_4 \tag{16d}$$

which are all based on t_{go}, and some also require τ_M, both of which are uncertain from the standpoint of the target. The navigation gain is constant for the PN and the APN guidance laws. Yet, it is time-varying in the OGL and the LQDG guidance laws. The navigation gain used by the interceptor is also uncertain from the standpoint of the target, thus it can be included in η.

Similar to the guidance law proposed in [10], and based on the structure of the classical guidance laws (15), we use the following structure for the guidance law of the interceptor:

$$u_M^k = \sum_{i=0}^{d} \mathbf{K}^{k-i}(\eta, t_{go}^{k-i}) \mathbf{x}^{k-i} \tag{17}$$

where d denotes delayed states, as we also consider the case that the pursuer uses delayed information regarding the state of the target. This structure is not limited to a specific guidance law, and it can also include switches between different guidance laws, as proposed, for example, in [9].

2. Information About The Interceptor's States

To accurately model the interceptor's guidance law, the target needs the information that the interceptor has about the entire state vector (3), including the relative states, the interceptor's own states, and the target's states. Clearly, this information is inaccessible to the target. In a similar fashion to the solutions presented above, the interceptor acquires this information from noisy and imperfect measurements using a state estimator. However, the target only has the statistical information provided by its own estimator. Therefore, as the true acceleration command of the

interceptor is unknown, the target needs to estimate it instead. Moreover, as the target cannot generally know what guidance law the pursuer uses, we assume that it has to identify it within a given set of admissible guidance laws. Therefore, we can model this estimate as

$$\hat{u}_M^k = \sum_{j=1}^{p^{\max}} P_j^k \sum_{i=0}^{d} \mathbf{K}^{k-i}(\eta, t_{go}^{k-i})\hat{\mathbf{x}}^{k-i} \tag{18}$$

where $p^{\max} = |\mathcal{P}|$, $P_j^k \triangleq Pr(p^k = j \mid \mathcal{Y}^k)$ is the mode probability conditioned on the measurement history, $\mathcal{Y}^k$, which can be obtained from a multiple model state estimator, such as the MMAE, and $\hat{\mathbf{x}}^{k-i} \sim p_{\hat{x}^{k-i}}$ for any $i = 0, \ldots, d$.

Example II.2. *Consider an interceptor that can select, at each time step, a guidance law from the set $\mathcal{P} = \{PN_3, PN_4, APN_3\}$, where PN_i stands for proportional navigation with navigation gain i and APN_3 stands for APN with navigation gain 3. The state estimator of the target provides statistical information about the interceptor's states, and the law of total probability yields*

$$p(\mathbf{x}_M^k \mid \mathcal{Y}^k) = \sum_{j=1}^{3} P_j^k p(\mathbf{x}_M^k \mid p^k = j, \mathcal{Y}^k). \tag{19}$$

Thus, the guidance law of the interceptor can be modeled as

$$\hat{u}_M^k = \sum_{i=0}^{k'-1-k} \left[P_1^k \frac{3(\hat{x}_{1|1}^k + \hat{x}_{2|1}^k i)}{i^2} + P_2^k \frac{4(\hat{x}_{1|2}^k + \hat{x}_{2|2}^k i)}{i^2} + P_3^k \frac{3(\hat{x}_{1|3}^k + \hat{x}_{2|3}^k i + \frac{1}{2}i^2 x_4^{k-d})}{i^2} \right] p_{t_{go}^k}(i) \tag{20}$$

where $\hat{x}_{i|j} \triangleq \mathbb{E}[x_i \mid p^k = j, \mathcal{Y}^k]$ is the current time conditional expectation of the ith state given the measurements and given that the jth mode is valid. Notice that x_4^k, which is the target acceleration, is perfectly known to the target but not to the interceptor. Thus, we replace the current time estimate with delayed information, x_4^{k-d}, as proposed in [10].

Determining $p_{\hat{x}^{k-i}}$ is not trivial, as this PDF represents the target's knowledge about the interceptor's knowledge of the entire state vector. The straightforward solution is to use the readily available outputs of the target's estimator, which are, clearly, different from the interceptor's

estimator's actual outputs. When considering the relative states, ξ and $\dot{\xi}$, no better information regarding these states is available to the target (however, if it does exist, then the target should use it in its state estimator). However, the target's information about the internal states, $\mathbf{q}_M$ and $\mathbf{q}_T$, differs drastically from the interceptor's information. The target has very accurate information regarding $\mathbf{q}_T$, which is unavailable to the interceptor. We can, for example, add artificial noises or use delayed data to model the inherent uncertainties of the interceptor's estimation process. In contradistinction, the target's information regarding $\mathbf{q}_M$ is significantly less accurate than the information the interceptor has, and there is very little the target can do about that. Obviously, if better information regarding any of the states, the dynamics, or the estimator of the interceptor is available, then it should be used.

These states evolve with time according to

$$\hat{\mathbf{x}}^{k+1} = \mathbf{F}^k(\eta)\hat{\mathbf{x}}^k + \mathbf{g}_M^k(\eta)\hat{u}_M^k + \mathbf{g}_T^k u_T^k + \hat{\omega}^k \tag{21}$$

where $\hat{\omega}^k$ is a white process noise with a known PDF $p_{\hat{\omega}^k}$, which models the unknown effects the target has about the information of the interceptor. For example, the noise about the target internal dynamics should be higher compared to ω^k, as explained above.

E. Performance Index

The cost function, which we aim to maximize in the evasion problem, is set to be

$$J \triangleq \mathbb{E}\left[g(\mathbf{x}^f)\right] \tag{22}$$

where $g(\cdot)$ is a convex and continuous objective function. The expectation is with respect to all the random variables presented above at the final step of the engagement, f, which is also random, and we assume that it exists. A detailed description of the evasion problem is presented in the sequel.

III. Optimal Evasion Structure

Providing new insight into the existence and structure of optimal evasion maneuvers in the stochastic scenarios discussed earlier, the following theorem presents the first and main result of this paper.

Theorem III.1. *At each time t^n, there exists at least one optimal control sequence for the evasion problem. Furthermore, of all optimal control sequences, at least one must possess the well-known bang-bang structure, that is*

$$\overset{\star}{u}_T^k \in \{-u_T^{\max}, u_T^{\max}\} \tag{23}$$

for all $k = n, \ldots, k' - 1$.

Thus, only the boundaries $-u_T^{\max}$ and $u_T^{\max}$ of the interval $[-u_T^{\max}, u_T^{\max}]$ need be considered at each time step, instead of the entire interval, which, clearly, significantly reduces the computational complexity of the optimal control problem. However, even this drastic reduction in computational complexity cannot bypass the curse of dimensionality, as it leaves us with exponential complexity. Furthermore, we note that Theorem III.1 clearly does not guarantee the uniqueness of any optimal evasion maneuver (including the bang-bang one).

Proof. For convenience of exposition, we first explicitly rewrite the evasion problem presented in the previous section. Ideally, we seek to find an evasion law in feedback form, which depends on the states, the time-to-go (or the final time of the engagement), and the uncertain parameters. Thus, from the standpoint of feedback implementation, this problem is formulated as a stochastic model predictive control problem, that is, we solve it for its entire horizon and then implement just the first control action. Notice that this is an infinite-dimensional problem, and its solution is generally

intractable. The evasion problem at each time step t^n is:

$$\max_{\{u_T^k\}_{k=n}^{k'-1}} \mathbb{E}\left[g(\mathbf{x}^f)\right] \tag{24a}$$

$$\text{s.t. } \mathbf{x}^{k+1} = \mathbf{F}^k(\eta)\mathbf{x}^k + \mathbf{g}_M^k(\eta)\hat{u}_M^k + \mathbf{g}_T^k u_T^k + \omega^k, \quad \forall k = n, \ldots, k' - 1, \tag{24b}$$

$$\mathbf{x}^n \sim p_{x^n}, \quad \eta \sim p_\eta, \quad \omega^k \sim p_{\omega^k}, \quad \forall k = n, \ldots, k' - 1, \tag{24c}$$

$$\hat{u}_M^k = \sum_{j=1}^{p^{\max}} P_j^k \sum_{i=0}^{d} \mathbf{K}^{k-i}(\eta, t_{go}^{k-i})\hat{\mathbf{x}}^{k-i}, \quad \forall k = n, \ldots, k' - 1, \tag{24d}$$

$$\hat{\mathbf{x}}^{k+1} = \mathbf{F}^k(\eta)\hat{\mathbf{x}}^k + \mathbf{g}_M^k(\eta)\hat{u}_M^k + \mathbf{g}_T^k u_T^k + \hat{\omega}^k, \quad \forall k = n, \ldots, k' - 1, \tag{24e}$$

$$\hat{\mathbf{x}}^{n-i} \sim p_{\hat{x}^{n-i}}, \quad \forall i = 0, \ldots, d, \quad \hat{\omega}^k \sim p_{\hat{\omega}^k}, \quad \forall k = n, \ldots, k' - 1, \tag{24f}$$

$$f \sim p_f(i), \quad t_{go}^k \sim p_{t_{go}^k}(i), \quad \forall i = 0, 1, \ldots, \infty, \quad \forall k = n - d, \ldots, k' \tag{24g}$$

$$|u_T^k| \leq u_T^{\max}, \quad \forall k = n, \ldots, k' - 1. \tag{24h}$$

To prove Theorem III.1, we rely on established findings from convex optimization theory [25, 26], and, in particular, on the following Theorem.

Theorem III.2 (Theorem 7.42 in [25]). *Let $J : S \to \mathbb{R}$ be a convex and continuous objective function over the convex and compact set $S \subseteq \mathbb{R}^n$. Then there exists at least one maximizer of J over S that is an extreme point of S.*

To employ III.2, we need to prove that the objective function of the evasion problem (24) is convex and continuous over its constraint set, which is convex and compact. It would then follow that the set of optimal evasion maneuvers is nonempty, and, at each time step, there exists an optimal solution in the set $\{-u_T^{\max}, u_T^{\max}\}$, i.e., an optimal solution having a bang-bang structure.

We proceed by proving the following two lemmas. The first lemma proposes that the constraint set is convex and compact. The second lemma establishes that the objective function is convex and continuous over the constraint set. The main Theorem then follows directly from Theorem III.2 and these two lemmas.

Lemma III.3. *Presented in Eqs.* (24b)–(24h), *the underlying constraint set of the evasion problem is convex and compact.*

Proof. The underlying set is presented in its functional form. If the functional form comprises affine functions for equality constraints and convex functions for non-positive inequality constraints, then this set, denoted as S in Theorem III.2, is convex [25, Ch. 8.1]. The equality constraints (24b), (24d), and (24e) can be substituted recursively to eliminate the state variables $\mathbf{x}^{n+1}, \ldots, \mathbf{x}^{k'}$ and the estimated guidance actions of the interceptor $\hat{u}_M^n, \ldots, \hat{u}_M^{k'-1}$, and the estimated state variables used by the interceptor $\hat{\mathbf{x}}^{n+1}, \ldots, \hat{\mathbf{x}}^{k'}$, respectively. Hence, the terminal state can be presented in the following manner:

$$\mathbf{x}^f(\mathbf{u}) = A^f \mathbf{u} + \mathbf{b}^f, \tag{25}$$

where $\mathbf{u} \triangleq [u_T^n, \ldots, u_T^{k'-1}]^\top$ is the vector that contains the target acceleration commands for the horizon, and $A_f, \mathbf{b}_f$ depend on the exogenous variables, such as η, $\{\omega^k\}_n^{k'-1}$, and $\mathbf{x}^n$, but not on $\mathbf{u}$. Thus, the underlying set can be expressed using only the target acceleration commands $\mathbf{u}$ and the terminal state $\mathbf{x}^f$. After eliminating the state variables, we remain with the constraints in (24h), that can be rewritten as $\left| u_T^k \right| - u_T^{\max} \leq 0$, that is, the underlying set is the hypercube $[-u_T^{\max}, u_T^{\max}]^{k'-n}$, which is convex and compact. ∎

We next prove that the objective function is both convex and continuous over the constraint set.

Lemma III.4. *Defined in Eq.* (24), *the objective function of the evasion problem is convex and continuous over the constraint set.*

Proof. Lemma III.3 shows that the underlying set of the evasion problem is convex, and, while proving it, we have established that only the target acceleration commands $u_T^n, \ldots, u_T^{k'-1}$ remain as free variables in this problem. Using (25), the objective function is the expected value of $g(\mathbf{x}^f) = g(A^f \mathbf{u} + \mathbf{b}^f)$, which preserves its convexity under linear change of variables [25, Theorem 7.17]. Moreover, the expectation operator preserves the convexity of $g(\cdot)$ as infinite summation and multiplication by nonnegative scalars also preserve convexity [26, Section 3.2.1]. The lemma then follows from observing that these operations also preserve continuity. ∎

14

As we have shown that the objective function is convex and continuous (Lemma III.4) over its convex and compact constraint set (Lemma III.3), our main result follows directly from Theorem III.2. ∎

IV. Terminal-Set-Based Evasion

This section leverages the bang-bang structure established earlier to obtain a practical evasion law with analytic evaluation based on terminal sets. The construction of these sets allows us to evaluate the resulting cost for the two extreme current commands $u_T^n \in \{\pm u_T^{\max}\}$ in closed form. To make use of these evaluations, we define a selector as a rule that maps the predicted terminal outcomes associated with the two admissible commands, $u_T^n = +u_T^{\max}$ and $u_T^n = -u_T^{\max}$, to the chosen control input at stage n. The resulting selector reduces the exponential search over future bang sequences to a single score comparison that determines the current acceleration command.

A. Scope and Assumptions

Consider the discrete-time stochastic endgame formulated in Sec. II. We denote n as the current decision step, k a generic stage, i a candidate terminal index, and f the random terminal index. The state is $\mathbf{x} \in \mathbb{R}^{n_x}$. We let $\mathbf{C} \in \mathbb{R}^{p \times n_x}$ be a fixed output-selection matrix that extracts the components of the terminal state relevant to the performance measure (e.g., miss distance). The terminal-time PMF is $p_f(i) = \mathbb{P}[f = i]$. The pursuer's guidance law is selected from $\mathcal{P} = \{p_j\}_{j=1}^{p^{\max}}$ with mode probabilities P_j^n at stage n. An estimator provides the necessary first and second moments; for example, the Kalman filter (KF) yields Gaussian posteriors, and the MMAE yields a Gaussian mixture model. The performance index instantiated here is a squared terminal cost,

$$g(\mathbf{x}^f) \;=\; \left\| \mathbf{C}\,\mathbf{x}^f \right\|^2, \tag{26}$$

rendering $g(\cdot)$ a convex and continuous cost, as assumed in Sec. II.E.

B. Terminal-Set Representation

For each index i in the support of the random terminal index f, that is, each candidate terminal step with $p_f(i) > 0$, and for each admissible guidance-law mode $j \in \{1, \ldots, p^{\max}\}$, unrolling the discrete-time closed-loop dynamics yields an affine dependence of the terminal state on the current command:

$$\mathbf{x}_i^f = \mathbf{a}^n(i, j)\, u_T^n + \mathbf{z}_{i,j}^n. \tag{27}$$

The vector $\mathbf{a}^n(i, j) \in \mathbb{R}^{n_x}$ is the input-to-terminal-state gain of the current evader command under mode p_j,

$$\mathbf{a}^n(i, j) \triangleq \mathbf{\Phi}(i, n+1; p_j)\, \mathbf{g}_T, \tag{28}$$

where the mode-conditioned state-transition product

$$\mathbf{\Phi}(i, \ell; p_j) \triangleq \mathbf{F}^{i-1}(\eta, p_j) \cdots \mathbf{F}^\ell(\eta, p_j), \qquad \mathbf{\Phi}(\ell, \ell; p_j) = \mathbf{I}_{n_x}, \tag{29}$$

maps states from stage ℓ to i. Here $\mathbf{F}^k(\eta, p_j)$ denotes the effective closed-loop dynamics matrix obtained from the open-loop matrix $\mathbf{F}^k(\eta)$ in Sec. II by substituting the pursuer's mode-p_j guidance law into the state-update equation. At the same time, the evader command still enters through $\mathbf{g}_T u_T^k$. Thus, any state delay or time-to-go dependence of the guidance law is embedded in $\mathbf{F}^k(\eta, p_j)$ and, in turn, in $\mathbf{\Phi}(\cdot; p_j)$.

The term $\mathbf{z}_{i,j}^n$ aggregates all contributions to the terminal state that do not depend on the current command u_T^n:

$$\mathbf{z}_{i,j}^n \triangleq \sum_{k=n+1}^{i-1} \mathbf{a}^k(i, j)\, u_T^k + \mathbf{d}_{i,j} + \mathbf{w}_{i,j}, \tag{30}$$

with input-to-terminal gains

$$\mathbf{a}^k(i, j) = \mathbf{\Phi}(i, k+1; p_j)\, \mathbf{g}_T, \qquad k = n+1, \ldots, i-1. \tag{31}$$

The vector $\mathbf{d}_{i,j}$ collects all known, deterministic contributions to the terminal state under mode

p_j, including the pursuer's closed-loop guidance inputs and any modeled exogenous terms. The term $\mathbf{w}_{i,j}$ aggregates all stochastic contributions to the terminal state under mode p_j, including the accumulated effects of process noise, measurement noise, and the propagated posterior-state uncertainty produced by the estimator (KF or MMAE). In particular, $\mathbf{w}_{i,j}$ represents the total uncertainty entering through the noise terms in the dynamics and their propagation through the estimator's moment updates, and is, therefore, distinct from the modeled stochasticity of the future evader inputs $\{u_T^k\}_{k>n}$.

For each (i, j), define the mean and covariance of $\mathbf{z}_{i,j}^n$,

$$\boldsymbol{\mu}_{i,j}^n \triangleq \mathbb{E}[\mathbf{z}_{i,j}^n], \qquad \boldsymbol{\Sigma}_{i,j}^n \triangleq \mathrm{Var}(\mathbf{z}_{i,j}^n), \tag{32}$$

which expand, without requiring independence assumptions, as

$$\boldsymbol{\mu}_{i,j}^n = \sum_{k=n+1}^{i-1} \mathbf{a}^k(i, j)\, m^k + \mathbf{d}_{i,j} + \mathbb{E}[\mathbf{w}_{i,j}], \tag{33a}$$

$$\boldsymbol{\Sigma}_{i,j}^n = \sum_{p=n+1}^{i-1} \sum_{q=n+1}^{i-1} \mathbf{a}^p(i, j)\, \mathrm{Cov}(u_T^p, u_T^q)\, \mathbf{a}^q(i, j)^\top + \mathrm{Var}(\mathbf{w}_{i,j}), \tag{33b}$$

where $m^k \triangleq \mathbb{E}[u_T^k]$ arises from the stochastic modeling of future evader inputs in the expectation evaluation. In particular, the controller optimizes only the current command u_T^n, while the future inputs $\{u_T^k\}_{k>n}$ are treated as random variables with a prescribed distribution used solely for evaluating the expected cost.

C. Evasion Law Derivation

The objective for the current decision is

$$J(u_T^n) \triangleq \mathbb{E}[g(\mathbf{x}^f)] = \sum_i p_f(i) \sum_{j=1}^{p^{\max}} P_j^n \, \mathbb{E}\left[\|\mathbf{C}\mathbf{x}_i^f\|^2 \,\Big|\, f = i, p_j\right]. \tag{34}$$

Using (27) and the quadratic identity for any finite second-moment $\mathbf{z}_{i,j}^n$, with $\| \cdot \|$ denoting the Euclidean norm,

$$\mathbb{E}\left[\left\| \mathbf{C}\big(\mathbf{a}^n(i,j)u_T^n + \mathbf{z}_{i,j}^n\big) \right\|^2 \right] = \left\| \mathbf{C}\big(\mathbf{a}^n(i,j)u_T^n + \boldsymbol{\mu}_{i,j}^n\big) \right\|^2 + \mathrm{tr}\big(\mathbf{C}\,\boldsymbol{\Sigma}_{i,j}^n\,\mathbf{C}^\top\big). \tag{35}$$

where tr denotes the trace. Note that only the mean term depends on u_T^n. Therefore, evaluating (34) at the two extreme commands gives the terminal-set scores

$$S_+^n \triangleq \sum_i p_f(i) \sum_{j=1}^{p^{\max}} P_j^n \left\| \mathbf{C}\big(\mathbf{a}^n(i,j)u_T^{\max} + \boldsymbol{\mu}_{i,j}^n\big) \right\|^2, \tag{36}$$

$$S_-^n \triangleq \sum_i p_f(i) \sum_{j=1}^{p^{\max}} P_j^n \left\| \mathbf{C}\big(-\mathbf{a}^n(i,j)u_T^{\max} + \boldsymbol{\mu}_{i,j}^n\big) \right\|^2. \tag{37}$$

Equivalently, define $\tilde{\mathbf{a}}_{i,j}^n \triangleq \mathbf{C}\mathbf{a}^n(i,j)$ and $\tilde{\boldsymbol{\mu}}_{i,j}^n \triangleq \mathbf{C}\boldsymbol{\mu}_{i,j}^n$, then

$$S_+^n - S_-^n = 4\,u_T^{\max} \sum_i p_f(i) \sum_{j=1}^{p^{\max}} P_j^n \left\langle \tilde{\mathbf{a}}_{i,j}^n, \tilde{\boldsymbol{\mu}}_{i,j}^n \right\rangle. \tag{38}$$

where $\langle a, b \rangle \triangleq a^\top b$. Define the shaping function

$$S_n = \sum_i p_f(i) \sum_{j=1}^{p^{\max}} P_j^n \left\langle \tilde{\mathbf{a}}_{i,j}^n, \tilde{\boldsymbol{\mu}}_{i,j}^n \right\rangle, \tag{39}$$

which aggregates, over all candidate terminal steps and guidance-law modes, the expected inner product between the input-to-terminal-state gain and the corresponding mean terminal shift. The function S_n encodes, in a single scalar, the net effect of choosing $u_T^n = \pm u_T^{\max}$ on the expected terminal cost, and its sign determines which extreme command is preferable. The obvious optimal choice is

$$\overset{\star}{u}_T^n = u_T^{\max}\,\mathrm{sgn}(S_n), \tag{40}$$

where $\mathrm{sgn}(\cdot)$ denotes the signum function.

We term this proposed evasion law the terminal-set-based evasion strategy, and use the shorthand notation TSE in the ensuing discussion.

D. Discussion

The terminal-set evaluation is analytical: once the posterior means and covariances (μ, Σ) are available from the estimator, the terminal-set scores in (36)-(37) and the associated cost $J(u_T^n)$ follow directly from closed-form expressions. In contrast to [22], no sequential MC is required for online use. The Gaussian assumption is consistent with the KF or MMAE posterior, and the latter provides the required mode-conditioned statistics and weights.

From a computational point of view, the method is lightweight. Let $N_f = \#\{\, i : p_f(i) > 0 \,\}$ be the number of terminal steps with positive probability, $p^{\max}$ the number of guidance-law modes, and $\bar{H} \triangleq \mathbb{E}[\, i - n \,]$ the average remaining horizon. Constructing the short-horizon transition products and input-to-terminal gains scales as $O(p^{\max} N_f \bar{H})$ for the mean terms and $O(p^{\max} N_f \bar{H}^2)$ for the covariance matrices. Online evaluation of the shaping function (39) then requires only $O(p^{\max} N_f n_x)$ operations per decision. The memory footprint is modest, limited to storing the precomputed terminal gains and corresponding moment statistics.

For comparison, the naive bang-bang MPC formulation in (24) explores on average $2^{\bar{H}}$ control branches per horizon step, yielding exponential complexity in $\bar{H}$. The terminal-set framework collapses this to near-linear scaling in the horizon, achieving orders-of-magnitude savings that make real-time stochastic evasion practical.

Finally, the control selector in (40) naturally retains the bang-bang structure: maximizing a convex terminal cost over the interval $[-u_T^{\max}, u_T^{\max}]$ attains an extreme point. Uncertainties in both terminal time and guidance law merely reweight the two terminal-set scores without altering this fundamental structure.

V. Numerical Evaluation

We illustrate the terminal-set-based selector on a planar lateral endgame with a single guidance mode.

A. Simulation Environment

The evader applies bounded lateral acceleration $u_T^k \in [-u_T^{\max}, u_T^{\max}]$ with $u_T^{\max} = 9g$. The pursuer uses PN with navigation constant $N = 3$. The sampling time is $\Delta t = 0.01$ s, and the closing speed is $V_c = 400$ m/s. Let the lateral state be $\mathbf{x}^k = \begin{bmatrix} \xi^k & \dot{\xi}^k \end{bmatrix}^\top$ and

$$\mathbf{x}^{k+1} = \underbrace{\begin{bmatrix} 1 & \Delta t \\ 0 & 1 \end{bmatrix}}_{\mathbf{F}} \mathbf{x}^k + \underbrace{\begin{bmatrix} \frac{(\Delta t)^2}{2} \\ \Delta t \end{bmatrix}}_{\mathbf{g}_T} u_T^k + \underbrace{\begin{bmatrix} \frac{(\Delta t)^2}{2} \\ \Delta t \end{bmatrix}}_{\mathbf{g}_M} u_M^k, \qquad \mathbf{C} = \begin{bmatrix} 1 & 0 \end{bmatrix}. \tag{41}$$

The terminal index is discretely uniformly distributed over the endgame window,

$$f \sim \mathrm{U}\{295, \ldots, 305\}, \quad N_f = 11. \tag{42}$$

This implies a final time span $t^f \in [2.95, 3.05]$ s and an associated initial range uncertainty $\rho^0 \approx V_c\, t^f \in [1180, 1220]$ m. For a candidate terminal index i, the PN acceleration is

$$u_M^k(i) = N\, \frac{\xi^k + t_{go}^k(i)\, \dot{\xi}^k}{\left(t_{go}^k(i)\right)^2}, \tag{43}$$

where $N = 3$, which induces the time-varying closed-loop matrices

$$\mathbf{F}^k(i) = \mathbf{F} + \mathbf{g}_M \begin{bmatrix} \dfrac{N}{(t_{go}^k(i))^2} & \dfrac{N}{t_{go}^k(i)} \end{bmatrix}, \qquad k = n, \ldots, i-1. \tag{44}$$

We select $\overset{\star n}{\hat{u}_T}$ by (40), and the corresponding analytic performance is

$$\mathbb{E}\left[\xi^2(t^f)\,\Big|\,\overset{\star n}{\hat{u}_T}\right] = \sum_i p_f(i)\left(\left\|\mathbf{C}\left(\mathbf{a}^n(i)\,\overset{\star n}{\hat{u}_T} + \boldsymbol{\mu}_i\right)\right\|^2 + \mathrm{tr}\left(\mathbf{C}\,\boldsymbol{\Sigma}_i\,\mathbf{C}^\top\right)\right). \tag{45}$$

B. Single Run: Confirming Bang-Bang Structure

To emphasize extremality, we model future evader commands as as an i.i.d. sequence with a uniform distribution, $u_T^k \sim \mathcal{U}[-u_T^{\max}, u_T^{\max}]$ for $k > n$. This changes only the variance to $\mathrm{Var}(u_T^k) = (u_T^{\max})^2/3$ and yields a quadratic cost

$$J(u_T^n) = \sum_i p_f(i)\left(\left\|\mathbf{C}\left(\mathbf{a}^n(i)\,u_T^n + \boldsymbol{\mu}_i\right)\right\|^2 + \mathrm{tr}\left(\mathbf{C}\,\boldsymbol{\Sigma}_i^{(\mathrm{unif})}\,\mathbf{C}^\top\right)\right), \tag{46}$$

which is maximized on the convex set $[-u_T^{\max}, u_T^{\max}]$ at the endpoints $\pm u_T^{\max}$.

Figure 2 illustrates the shape of the expected cost $J(u_T^n)$ under the assumption that future evader inputs are uniformly distributed. The curve is strictly convex, with maximum value achieved at the control bounds $u_T^{\max}$. This demonstrates, analytically and numerically, that the optimal command is bang-bang, even without explicitly assuming a bang-bang structure; thus, validating, for this example, the theoretical extremality result of Theorem III.1.

C. Monte Carlo Study

We next conduct an MC study to compare the proposed TSE policy against three classical stochastic evasion models: the RTS, Singer, and weaving models. Each simulation models a planar lateral engagement governed by the discrete-time dynamics (41) with sampling time $\Delta t = 0.01$ s, closing speed $V_c = 400$ m/s, and a proportional navigation pursuer with a navigation constant $N = 3$. The evader and pursuer accelerations are limited to $u_T^{\max} = 9g$ and $u_M^{\max} = 27g$, respectively.

A total of $N_{\mathrm{MC}} = 10{,}000$ independent trials are executed. In each trial, the true terminal index f is drawn from the discrete support defined in (42). The initial state of the engagement is sampled
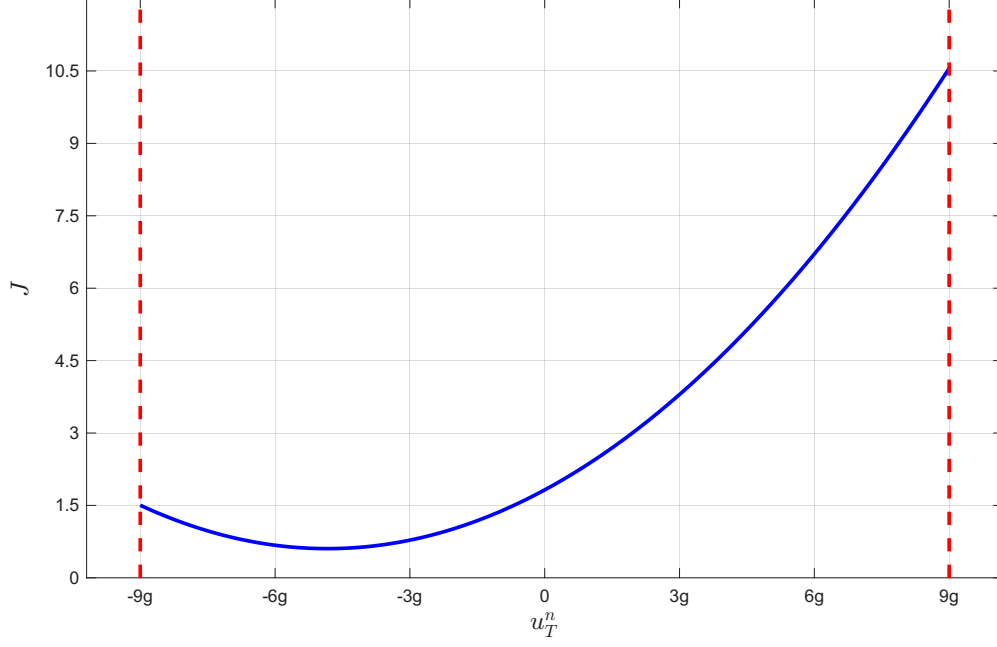
21

Fig. 2 Expected cost $J(u_T^n)$ under uniform future input model. The optimal control lies at the control bounds, confirming the bang-bang structure.

from a zero–mean Gaussian distribution,

$$\mathbf{x}^0 \sim \mathcal{N}(\mathbf{0}, P^0), \qquad P^0 = \text{diag}(100, 4), \tag{47}$$

so that both the initial lateral offset and relative velocity vary randomly across trials.

The measurement model is

$$y^k = \mathbf{C}\mathbf{x}^k + v^k, \qquad \mathbf{C} = \begin{bmatrix} 1 & 0 \end{bmatrix}, \tag{48}$$

where $v^k \sim \mathcal{N}(0, R_k)$ represents LOS angle jitter mapped into lateral-position noise. The measurement noise variance is not based on the true time-to-go but on a nominal one corresponding to the mean of the terminal-time distribution, ensuring that the estimator operates without access to the actual engagement duration. Specifically,

$$R_k = \left(\sigma_\lambda V_c t_{go}^{k,\text{nom}}\right)^2, \qquad \sigma_\lambda = 5 \text{ mrad}, \tag{49}$$

22

where $t_{go}^{k,\text{nom}} = (\bar{f} - k)\Delta t$ and $\bar{f} = \mathbb{E}[f] \approx 300$ for the chosen support (42). The process noise covariance is defined as

$$Q_k = (u_T^{\max})^2 \, \mathbf{g}_T \mathbf{g}_T^\top. \tag{50}$$

Both sides employ identical KFs as state estimators. To model its information advantage, the pursuer is initialized with a smaller covariance,

$$P_M^0 = \beta P_T^0, \qquad \beta = 0.25, \tag{51}$$

indicating that the pursuer's initial uncertainty is smaller than the evader's. Moreover, we assume that both agents know each other's acceleration commands, which is conservative from the evader's perspective. On the target's side, this assumption is reasonable: as shown in [7], the pursuer's guidance law can be identified using an MMAE filter, allowing the target to reconstruct its acceleration commands. The converse, however, has not been established, as the authors are not aware of any proof or demonstration that the pursuer can estimate the target's stochastic maneuver commands. Imposing this assumption on the pursuer, therefore, benefits the pursuer and makes the evasion problem more challenging for the target, rendering our simulation results conservative.

During each simulation, the pursuer computes its proportional navigation acceleration command (43) using the estimates and the mean value for the time-to-go. This command is saturated to $\pm u_M^{\max}$. The evader acceleration u_T^n depends on the evasion strategy under test. For the proposed TSE case, the terminal–set shaping function S_n from (39) is evaluated at each step, and the evader applies the bang–bang command (40). In the RTS case, the evader alternates between $\pm u_T^{\max}$, with switching times drawn from an exponential distribution of rate $1/3$ s^{-1}. In the Singer case, the evader follows a first–order Gauss–Markov acceleration process $\dot{a}_T = -(1/\tau)a_T + w_a$ with $\tau = 1$ s and $\sigma_a = u_T^{\max}/2$, truncated to the control bounds. In the weaving case, the evader executes a deterministic sinusoidal maneuver $a_T(t) = u_T^{\max} \sin(\pi t + \pi/2)$, producing continuous oscillatory motion.

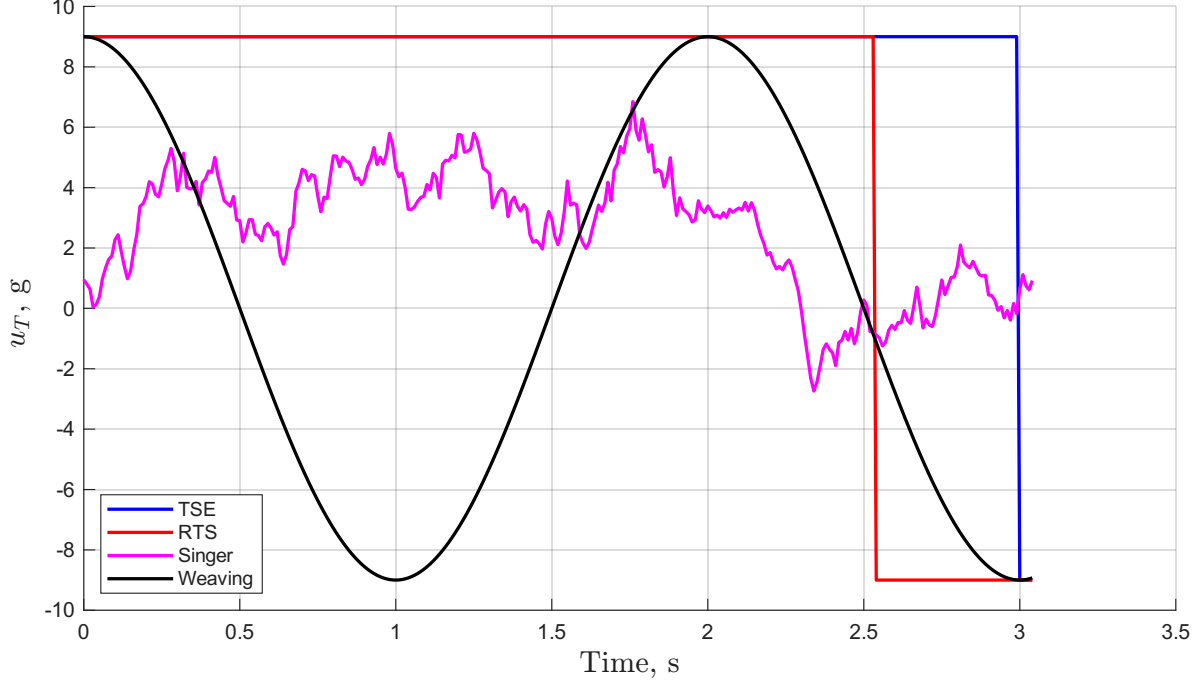Figure 3 illustrates the evader acceleration profiles for a representative engagement under all four

Fig. 3   Evader acceleration command profiles for a representative engagement under the TSE (blue line), RTS (red line), Singer (magenta line), and weaving (black line) evasion strategies.

strategies. For this scenario, the resulting miss distances are 6.29 m for TSE, 5.04 m for RTS, 1.93 m for Singer, and 0.63 m for weaving. These differences can be directly related to the qualitative behavior of the evasion laws. The bang-bang nature of the TSE law, the randomized sign changes produced by RTS, the correlated stochastic fluctuations generated by the Singer model, and the periodic structure of the weaving maneuver are clearly visible. Although TSE, RTS, and weaving all begin and end at the same acceleration values, their switching patterns are fundamentally different. In particular, both the presence of switching and the timing of the switch instants play a critical role in shaping the terminal lateral displacement. The TSE strategy places its switches at advantageous stages of the engagement to amplify the miss distance, whereas RTS switches at statistically random times and therefore achieves a smaller displacement despite using the same control bounds.

Figure 4 compares the empirical CDFs of $|\xi(t^f)|$ across the four strategies ensemble of 10,000 trials. A larger miss distance indicates improved evasion performance; therefore, higher values correspond to better outcomes for the evader. The two bang-bang profiles, TSE and RTS, clearly outperform the stochastic smooth maneuvers (Singer and weaving), achieving higher miss distances
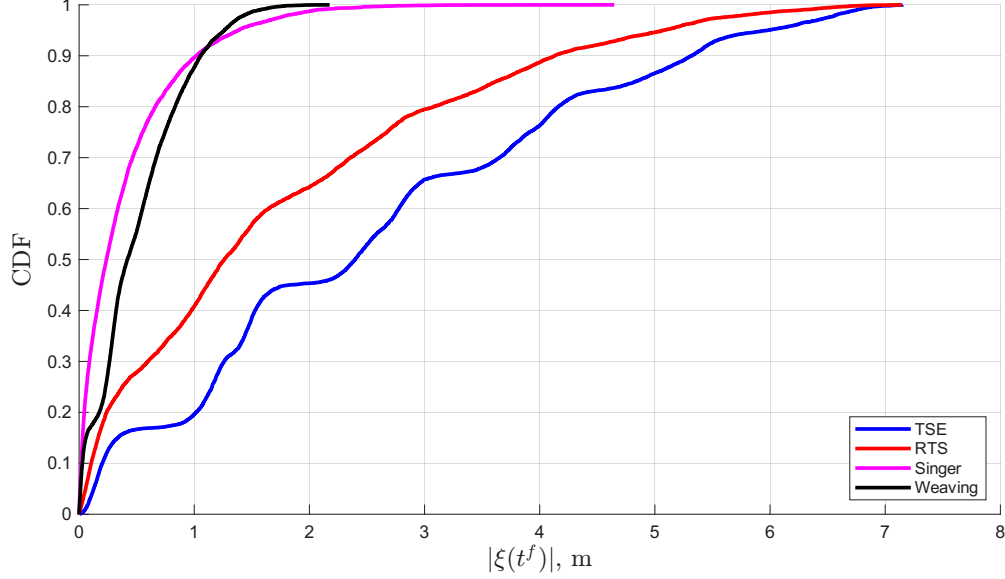
24

Fig. 4   Empirical CDF of miss distance across 10,000 MC trials using the TSE (blue line), RTS (red line), Singer (magenta line), and weaving (black line) evasion strategies.

across nearly the entire distribution. Notably, TSE consistently dominates RTS, producing larger evasive separations for all quantiles. For example, suppose the interceptor is equipped with a warhead having a lethality radius of 1 m. In that case, its single-shot kill probability (SSKP) against a target using either the Singer or weaving evasion maneuvers is about 0.9. In contradistinction, its SSKP against a target employing the bang-bang RTS evasion model is 0.4, and its SSKP against a target employing the TSE evasion maneuver is only 0.2 (requiring more than 10 independent interceptors to guarantee a kill probability of 0.9).

Table 1 reports summary statistics including the mean, median, and the 5th, 20th, 80th, and 95th percentiles. The TSE yields the highest mean and median final miss, along with the widest spread across the 5th to 95th percentiles. This confirms that TSE not only preserves extremality but also surpasses traditional stochastic maneuver models in effectiveness under uncertainty.

VI. Conclusions

This work addresses the problem of optimal evasion from an interceptor guided by a linear feedback law in the presence of uncertainty and bounded controls. Extending classical results from deterministic to stochastic settings, we prove that, under the GST guidelines, there always exists an

Table 1   Summary statistics of the miss distance $|\xi(t^f)|$ in m, including the mean, median, and the 5th, 20th, 80th, and 95th percentiles, for each evasion strategy.

Strategy	Mean	Median	P5	P20	P80	P95
TSE	2.55	2.4	0.13	1.02	4.16	5.98
RTS	1.75	1.26	0.06	0.24	3.08	5.08
Singer	0.4	0.24	0.01	0.05	0.66	1.38
Weaving	0.51	0.42	0.01	0.18	0.83	1.26

optimal evasion policy with a bang-bang structure. This structural result enables a dramatic reduction in the search space for optimal strategies: rather than optimizing over an infinite-dimensional input space, it suffices to consider binary-valued inputs at each time step.

Although this result reduces the formal dimensionality of the problem, solving for the optimal strategy remains computationally challenging due to the exponential growth in the number of binary control sequences with the planning horizon. To mitigate this, we introduce terminal-set-based evasion (TSE), a tractable closed-loop method that exploits the bang-bang structure in a stochastic decision-making framework. We evaluate the TSE strategy against three widely used stochastic evasion models: random telegraph signals, Singer processes, and weaving. In comparison, the TSE demonstrates its effectiveness by generating the largest miss distances. MC simulation results provide quantitative evidence of the method's effectiveness and confirm that the proposed evasion law achieves the intended improvements in evasion performance.

References

[1] Zarchan, P., *Tactical and Strategic Missile Guidance, Sixth Edition*, American Institute of Aeronautics and Astronautics, Inc., Washington, DC, 2012, Chaps. 6, 8, 20. https://doi.org/10.2514/4.868948.

[2] Ben-Asher, J. Z., and Yaesh, I., *Advances in Missile Guidance Theory*, Progress in astronautics and aeronautics: vol. 180, Reston, Va, 1998, Chap. 4.

[3] Shinar, J., and Steinberg, D., "Analysis of Optimal Evasive Maneuvers Based on a Linearized Two-Dimensional Kinematic Model," *Journal of Aircraft*, Vol. 14, No. 8, 1977, pp. 795–802. https://doi.org/10.2514/3.58855.

[4] Ben-Asher, J. Z., and Cliff, E. M., "Optimal Evasion Against a Proportionally Guided Pursuer," *Journal of Guidance, Control, and Dynamics*, Vol. 12, No. 4, 1989, pp. 598–600. https://doi.org/10.2514/3.20450.

[5] Shinar, J., Rotsztein, Y., and Bezner, E., "Analysis of Three-Dimensional Optimal Evasion with Linearized Kinematics," *Journal of Guidance and Control*, Vol. 2, No. 5, 1979, pp. 353–360. https://doi.org/10.2514/3.55889.

[6] Shima, T., "Optimal Cooperative Pursuit and Evasion Strategies Against a Homing Missile," *Journal of Guidance, Control, and Dynamics*, Vol. 34, No. 2, 2011, pp. 414–425. https://doi.org/10.2514/1.51765.

[7] Fonod, R., and Shima, T., "Multiple Model Adaptive Evasion Against a Homing Missile," *Journal of Guidance, Control, and Dynamics*, Vol. 39, No. 7, 2016, pp. 1578–1592. https://doi.org/10.2514/1. G000404.

[8] Shima, T., Oshman, Y., and Shinar, J., "Efficient Multiple Model Adaptive Estimation in Ballistic Missile Interception Scenarios," *Journal of Guidance, Control, and Dynamics*, Vol. 25, No. 4, 2002, pp. 667–675. https://doi.org/10.2514/2.4961.

[9] Turetsky, V., and Shima, T., "Target Evasion from a Missile Performing Multiple Switches in Guidance Law," *Journal of Guidance, Control, and Dynamics*, Vol. 39, No. 10, 2016, pp. 2364–2373. https://doi.org/10.2514/1.G000461.

[10] Shaferman, V., "Near-Optimal Evasion from Pursuers Employing Modern Linear Guidance Laws," *Journal of Guidance, Control, and Dynamics*, 2021, pp. 1–13. https://doi.org/10.2514/1.G005725.

[11] Hexner, G., Weiss, H., and Dror, S., "Temporal Multiple Model Estimator for a Maneuvering Target," *AIAA Guidance, Navigation and Control Conference and Exhibit*, 2008, p. 7456. https://doi.org/10.2514/6.2008-7456.

[12] Du, Q., Hu, Y., Jing, W., and Gao, C., "Three-dimensional target evasion strategy without missile guidance information," *Aerospace Science and Technology*, Vol. 157, 2025, p. 109857. https://doi.org/10.1016/j.ast.2024.109857.

[13] Hou, L., and He, S., "Optimal Evasive Guidance against Linear Optimal Guidance Laws," *IEEE Transactions on Aerospace and Electronic Systems*, 2025, pp. 1–16. https://doi.org/10.1109/TAES.2025. 3619914.

[14] Witsenhausen, H. S., "Separation of Estimation and Control for Discrete Time Systems," *Proceedings of the IEEE*, Vol. 59, No. 11, 1971, pp. 1557–1566. https://doi.org/10.1109/PROC.1971.8488.

[15] Striebel, C., "Sufficient statistics in the optimum control of stochastic systems," *Journal of Mathematical Analysis and Applications*, Vol. 12, No. 3, 1965, pp. 576–592. https://doi.org/10.1016/0022-247X(65) 90027-2.

[16] Zarchan, P., "Representation of Realistic Evasive Maneuvers by the Use of Shaping Filters," *Journal of Guidance, Control, and Dynamics*, Vol. 2, No. 4, 1979, pp. 290–295. https://doi.org/10.2514/3.55877, URL https://arc.aiaa.org/doi/10.2514/3.55877.

[17] Singer, R., "Estimating Optimal Tracking Filter Performance for Manned Maneuvering Targets," *IEEE Trans. Aerosp. Electron. Syst.*, Vol. AES-6, No. 4, 1970, pp. 473–483. https://doi.org/10.1109/TAES. 1970.310128.

[18] Yanushevsky, R., "Analysis of Optimal Weaving Frequency of Maneuvering Targets," *Journal of Spacecraft and Rockets*, Vol. 41, No. 3, 2004, pp. 477–479. https://doi.org/10.2514/1.6459.

[19] Marks, G., "Multiple Model Adaptive Estimation for Improving Guidance Performance Against Weaving Targets," *AIAA Guidance, Navigation, and Control Conference and Exhibit*, American Institute of Aeronautics and Astronautics, Keystone, Colorado, 2006. https://doi.org/10.2514/6.2006-6697.

[20] Weiss, M., "Robust Analysis of Guidance Performance Against Weaving Targets," *AIAA Guidance, Navigation and Control Conference and Exhibit*, American Institute of Aeronautics and Astronautics, Honolulu, Hawaii, 2008. https://doi.org/10.2514/6.2008-6495.

[21] Ratnoo, A., "Three-Point Guidance for Intercepting Weaving Targets," *Journal of Guidance, Control, and Dynamics*, Vol. 39, No. 8, 2016, pp. 1879–1884. https://doi.org/10.2514/1.G001718.

[22] Shaviv, I. G., and Oshman, Y., "Estimation-Guided Guidance and Its Implementation via Sequential Monte Carlo Computation," *Journal of Guidance, Control, and Dynamics*, Vol. 40, No. 2, 2017, pp. 402–417. https://doi.org/10.2514/1.G000360.

[23] Mudrik, L., and Oshman, Y., "Terminal-Set-Based Optimal Stochastic Guidance," *2023 31st Mediterranean Conference on Control and Automation (MED)*, 2023, pp. 653–658. https://doi.org/10.1109/MED59994.2023.10185736.

[24] Rusnak, I., "Optimal Guidance Laws with Uncertain Time-of-Flight," *IEEE Transactions on Aerospace and Electronic Systems*, Vol. 36, No. 2, 2000, pp. 721–725. https://doi.org/10.1109/7.845272.

[25] Beck, A., *Introduction to Nonlinear Optimization*, MOS-SIAM Series on Optimization, Society for Industrial and Applied Mathematics, 2014, Chaps. 7,8. https://doi.org/10.1137/1.9781611973655.

[26] Boyd, S., and Vandenberghe, L., *Convex optimization*, Cambridge university press, 2004, Chap. 3. https://doi.org/10.1017/CBO9780511804441.